

# Spectrum Reuse with Power Control for Two-Tier Femtocell Networks

Youngju Kim<sup>1</sup>, Hano Wang<sup>2</sup>, and Daesik Hong<sup>3</sup>

<sup>1</sup> Samsung Electronics / Hwasung, Korea yj1205.kim@saumsung.com

<sup>2</sup> Information and Telecommunication Engineering, Sangmyung University / Cheonan, Korea hhwang@smu.ac.kr

<sup>3</sup> School of Electrical and Electronic Engineering, Yonsei University / Seoul, Korea daesikh@yonsei.ac.kr

\* Corresponding Author: Daesik Hong

Received January 15, 2014; Revised March 17, 2014; Accepted July 28, 2014; Published October 31, 2014

\* Regular Paper

**Abstract:** This paper considers two-tier networks consisting of macrocells and femtocells operating in the same spectrum. This paper proposes a femtocell spectrum reuse scheme that determines the shared spectrum and transmit power for the femtocells to mitigate the effects of cross-tier interference between the macrocells and femtocells. The proposed scheme provides macrocell throughput that is unaffected by the increasing number of femtocells per cell site and improves the femtocell signal quality at the same time by limiting the cross-tier interference. This study analyzed the per-tier signal-to-interference ratio (SIR) and outage probability of the proposed scheme to investigate the macrocell and femtocell performance. The total throughput of the proposed scheme was analyzed based on the outage probabilities. The analysis and numerical results proved that high femtocell throughput can be achieved using only a small fraction of the spectrum while protecting the macrocell throughput. As a result, an improved total throughput was achieved enforcing higher spatial reuse.

**Keywords:** Femtocell, Cross-tier interference, Spectrum reuse, Femtocell power

## 1. Introduction

Achieving high capacity is a principal aim of wireless operators, who often encounter small regions of high demand within a large cell coverage area. The concept of femtocells is one architectural solution for these situations. A femtocell serves as a low power, short range data access point that provides improved indoor coverage to home users, while backhauling their traffic over the internet protocol network [1, 2]. Two-tier femtocell networks are considered a promising option for mobile operators to improve coverage and provide high-data-rate services in a cost-effective manner [3].

Previous studies of this topic investigated the capacity of two-tier femtocell networks [2, 4, 5]. The research shows that cross-tier interference leads to a decline in the macrocell and femtocell capacity in the absence of interference management. The influences of cross-tier interference are even worse for macrocell users than for femtocell users. Therefore, the handling cross-tier interference is a key technical challenge in two-tier

femtocell networks. As a way of managing cross-tier interference, Claussen employed an open access [6, 7]. Although open access can reduce the cross-tier interference, it causes problems in the network overhead and home user quality-of-service (QoS) [1]. By employing closed access, Chandrasekhar and Andrews assigned the orthogonal spectrum resources between the central macrocell and femtocell BSs to eliminate cross-tier interference [8]. On the other hand, considering the scarcity of the spectrum resources, spectrum sharing appears preferable because it increases the spectral efficiency through spatial frequency reuse. Recent studies consider spectrum sharing between macrocells and femtocells, which operate in the same spectrum, using closed access or partially open channel access [9-11].

In existing macrocellular networks, the same set of frequency channels is reused in another cell for which coverage is not overlapped. By effectively setting the reuse distance, spectrum utilization can be improved [12-14]. In two-tier networks, however, the same frequency channels can be reused by different networks within the same cell

site. This complicates the problem of spectrum reuse in two-tier networks.

The problem of spectrum reuse between macrocells and femtocells is simplified as a problem of the spectrum reuse of femtocells under constraints by assuming the macrocell as the primary infrastructure. This paper proposes a spectrum reuse scheme that allocates the spectrum that will be shared by femtocells among the entire spectrum already occupied by macrocells and the femtocell transmit power with the following objectives: 1) limit cross-tier interference to the macrocell, and 2) improve femtocell signal quality under interference from the macrocells. The per-tier signal-to-interference ratio (SIR) and outage probability of the proposed scheme were analyzed to investigate the macrocell and femtocell performance. Based on the outage probabilities, the total throughput of the proposed two-tier network was examined. The results showed that the total throughput with a given number of femtocells per cell site can be maximized by managing the spectrum reuse parameter.

## 2. System Model

### 2.1 Network and Channel Model

The macrocell network consists of  $N_c$  macrocells, where each macrocell occupies a hexagonal region with radius  $R_c$ . Inside each cell site, macrocell users are assumed to be distributed uniformly, and are served by orthogonal frequency division multiple access (OFDMA) [15]. In an OFDMA symbol, a subchannel is assigned randomly to one macrocell user. The entire bandwidth is shared by all macrocells.

A macrocell is overlaid with femtocells with radius  $R_f$ . Each femtocell accesses a random subset of the shared subchannels independent of the other femtocells, whereby each subchannel is accessed with equal probability [8]. The number of cochannel femtocells per frequency subchannel per cell site is represented as  $N_f$ . Femtocells provide closed access to a fixed set of subscribed indoor users and assign randomly a subchannel to one femtocell user [7].

The channel model consisting of a deterministic distance-dependent path-loss component and a random distance-independent were considered [16]. In particular, it was assumed that a signal transmitted at power  $P_t$  is received with an average power  $P_r$  according to

$$P_r = P_t \Psi_{r,t} D_{r,t}^{-\alpha}, \quad (1)$$

where  $D_{r,t}$  is the distance between the transmitter and receiver, and  $\alpha$  is the path-loss exponent. The distance-independent channel gain  $\Psi_{r,t}$  denotes the lognormal shadow fading with a mean of 0 dB and a standard deviation of  $\sigma_{r,t}$ , where shadow fading is usually characterized in terms of its dB spread as

$\sigma_{r,t} = \frac{\ln 10}{10} \sigma_{r,t,\text{dB}}$ . Shadow fading is assumed to be an independent across channel and independent of the transmitter and receiver positions. For simplicity, the background thermal noise is ignored because the noise contribution is minimal in an interference-limited network [18].

### 2.2. Signal Model

Assume that the central macrocell BS  $c_0$  is placed at the origin, and is transmitting to its desired user  $c$  with transmit power  $P_c$ . According to (1), the received signal power at the macrocell user can be expressed as

$$S_c = P_c \Psi_{c,c_0} D_{c,c_0}^{-\alpha}, \quad (2)$$

where  $\Psi_{c,c_0}$  is distributed according to  $LN(0, \sigma_{c,c_0}^2)$ . In the downlink, it is assumed that the macrocell user experiences interference from  $N_c - 1$  macrocell BSs  $c_j$ . Using the notations in (1), the expression for the aggregated macrocell interference for macrocell user  $c$  is given by the following:

$$I_{c,c} = \sum_{j=1}^{N_c-1} P_c \Psi_{c,c_j} D_{c,c_j}^{-\alpha}, \quad (3)$$

where the same fixed transmit power  $P_c$  for macrocell BSs is assumed. The random variable (RV)  $\Psi_{c,c_j}$  is distributed according to  $LN(0, \sigma_{c,c}^2)$ . The macrocell user also experiences interference from  $N_f$  femtocell BSs  $f_i$ . The aggregated femtocell interference for the macrocell user can be expressed as

$$I_{c,f} = \sum_{i=0}^{N_f-1} W P_{f_i} \Psi_{c,f_i} D_{c,f_i}^{-\alpha}, \quad (4)$$

where  $P_{f_i}$  is the transmission power of the femtocell BS  $f_i$  and  $D_{c,f_i}$  represents the distance between femtocell BS  $f_i$  and macrocell user  $c$ . The RV  $\Psi_{c,f_i}$  is distributed as  $LN(0, \sigma_{c,f}^2)$ . The constant  $W$  is used to take the wall penetration loss into account [4, 8]. In particular, we represent the interference from the femtocell BS  $f_i$  received at the macrocell user as  $I_{c,f_i} = W P_{f_i} \Psi_{c,f_i} D_{c,f_i}^{-\alpha}$ . The received interference from the femtocell BSs in the neighboring macrocell area is assumed to be negligible due to large path loss [17].

Within the coverage area of  $c_0$ , the femtocell BS  $f_0$  is communicating with its desired user  $f$  at power  $P_{f_0}$  using the same channel as  $c_0$ . The received signal power at the femtocell user is expressed as

$$S_f = P_{f_0} \Psi_{f,f_0} D_{f,f_0}^{-\beta}, \quad (5)$$

where  $\Psi_{f,f_0}$  is distributed as  $LN(0, \sigma_{f,f_0}^2)$  and  $\beta$  is the indoor path-loss exponent. The received interference from the cochannel macrocell BSs is expressed as

$$I_{f,c} = \sum_{j=0}^{N_c-1} W P_c \Psi_{f,c_j} D_{f,c_j}^{-\alpha}, \quad (6)$$

where  $\Psi_{f,c_j}$  is distributed as  $LN(0, \sigma_{f,c}^2)$ . In particular, the received interference from the central macrocell BS  $c_0$  is represented as  $I_{f,c_0} = P_c \Psi_{f,c_0} D_{f,c_0}^{-\alpha}$ . The aggregated femtocell interference for the femtocell user can be expressed as

$$I_{f,f} = \sum_{i=1}^{N_f-1} W^2 P_{f_i} \Psi_{f,f_i} D_{f,f_i}^{-\alpha}, \quad (7)$$

where  $\Psi_{f,c_j}$  is distributed as  $LN(0, \sigma_{f,f}^2)$ . For simplicity, the background thermal noise will be ignored because the noise contribution is minimal in an interference-limited network [18].

### 3. Spectrum Reuse with Power Control for Femtocells

Considering the macrocell as the primary infrastructure, this paper proposes a spectrum reuse scheme that adequately allocates the spectrum and the transmit power for femtocells with the following objectives: 1) limit cross-tier interference to the macrocell, and 2) improve femtocell signal quality under interference from the macrocells. This section presents the proposed spectrum reuse scheme for achieving those objectives.

The principle of the proposed spectrum reuse scheme is to degrade the macrocell SIR performance for users that already have more than adequate signal quality while protecting those users that suffer from poor signal quality. Accordingly, femtocells preferentially reuse the macrocell subchannels with superior signal quality, which are typically occupied by the macrocell users close to the cell center in a downlink. These subchannels are represented by virtually partitioning the macrocell area into two nonoverlapping concentric areas: the inner region and outer region. The inner region is characterized by its radius  $r$ . The frequency subchannels used in the inner region are reused by femtocells. The set of the reused subchannels is represented by  $B_{in}$ , which is a subset of the entire set of frequency subchannels,  $B$ . Fig. 1 gives an example of interference scenario and the spectrum use of the proposed scheme.

Femtocells can provide superior signal quality to their users because of their short transmit-receive distance. On the other hand, femtocells close to the macrocell BS in

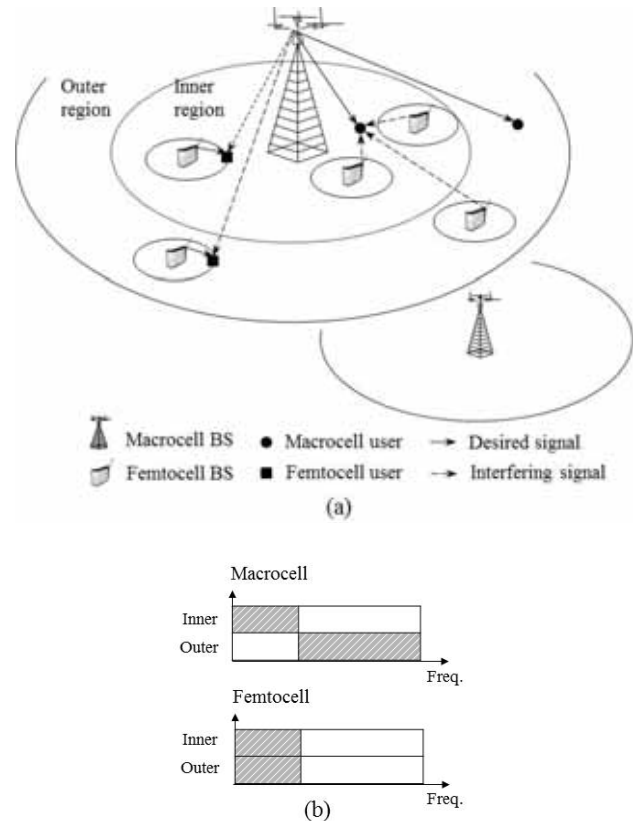


Fig. 1. Description of the proposed spectrum reuse scheme (a) downlink interference scenario, (b) an example of spectrum use (logical frequency channel model).

particular experience severe interference from macrocell transmissions in a downlink. To avoid such interference, in [19], the femtocells in the inner region were assigned different channels that are not used in the macrocell by assuming that the macrocell network employs a reuse factor greater than one. Rather than assigning orthogonal channels to the femtocells, this paper proposes the use of interference cancellation (IC) for the femtocell receivers in the inner region, where it has been proven that IC is highly preferable for the disparate power levels of the macrocell and femtocell [20, 21]. In doing so, the femtocell signal quality can be improved without a loss of spectral efficiency.

In the two-tier network, the same channels are reused by different networks in the same cell site. Macrocell users might be affected by severe femtocell interference in the proximity of the densely distributed cochannel femtocells, even though the reused spectrum is limited. To complement the strategy of spectrum limitation and employ IC for the femtocells, this paper proposes that femtocells curb their transmit power according to these power constraints:

- The ratio of cross-tier interference to the macrocell desired signal power for a macrocell user is limited to a defined level, irrespective of the number of femtocells, i.e.,  $I_{c,f} / S_c < T_1$ , where the individual interference from a femtocell BS  $f_0$  is limited by

$$I_{c,f_0} / S_c < T_1 / N_f.$$

- The ratio of the femtocell desired signal power to the dominant macrocell interference power for a femtocell user is limited to guarantee IC performance by  $S_f / I_{f,c_0} < T_2$  for the femtocells in the inner region.

Assuming the maximum transmit power limitations on the femtocell power,  $P_{f,max}$ , the transmit power of the femtocell BS  $f_0$  maximizing its own SIR is given by the minimum of the boundary values determined using the above constraints as follows:

$$P_{f_0} = \begin{cases} \min \left( P_{f,max}, \frac{S_c T_1}{W \Psi_{c,f_0} D_{c,f_0}^{-\alpha} N_f} \right), & \text{outer} \\ \min \left( P_{f,max}, \frac{S_c T_1}{W \Psi_{c,f_0} D_{c,f_0}^{-\alpha} N_f}, \frac{I_{f,c_0} T_2}{\Psi_{f,f_0} D_{f,f_0}^{-\beta}} \right), & \text{inner} \end{cases} \quad (8)$$

#### 4. Performance Analysis of the Two-Tier Network

The performance of the two-tier network employing the proposed spectrum reuse scheme was evaluated. At this stage, the per-tier outage probability and throughput performances are analyzed. Because the spectrum reuse scheme is characterized by the radius,  $r$ , the per-tier outage probabilities according to  $r$  is derived. The next step is to derive the total throughput of this system using the outage probabilities. By analyzing the total throughput of the considered two-tier network, the results show that the throughput can be maximized using the proposed scheme with the given number of femtocells per cell site.

##### 4.1 Per-tier Outage Probability Analysis

###### 4.1.1 Femtocell Outage Probability

Consider a femtocell user in the outer region served by the femtocell BS  $f_0$ . The transmit power of  $f_0$  is denoted by  $P_{f_0}$ , which is given in (8). The received SIR at the femtocell user is expressed as

$$SIR_{f,out} = \frac{S_f}{I_{f,c} + I_{f,f}} = \frac{P_{f_0} \Psi_{f,f_0} D_{f,f_0}^{-\beta}}{\sum_{j=0}^{N_c-1} P_c \Psi_{f,c_j} D_{f,c_j}^{-\alpha}}, \quad (9)$$

where it is assumed that  $I_{f,f}$  is insignificant, because the propagation between femtocells suffers at least double wall partition losses [5, 17].

To compute the distribution of the  $SIR_{f,out}$ , the distribution of  $P_{f_0}$  is first derived. From (8),  $P_{f_0}$  in the

outer region is given by

$$P_{f_0} = \min \left( P_{f,max}, \frac{S_c T_1}{W \Psi_{c,f_0} D_{c,f_0}^{-\alpha} N_f} \right). \quad (10)$$

We define  $X$  and  $Y$  as

$$X = P_{f,max}, \quad Y = \frac{P_c \Psi_{c,c_0} D_{c,c_0}^{-\alpha} T_1}{W \Psi_{c,f_0} D_{c,f_0}^{-\alpha} N_f}, \quad (11)$$

where  $X$  is a fixed constant and  $Y$  is a lognormal random variable (RV). Using the definitions of  $X$  and  $Y$ , (10) can be expressed as  $P_{f_0} = \min(X, Y)$ . The cumulative distribution functions (CDF) of  $X$  and  $Y$ , which are denoted by  $F_X(x)$  and  $F_Y(y)$ , respectively, can be expressed as

$$F_X(x) = H(x - P_{f,max}),$$

$$F_Y(y) = 1 - Q \left( \frac{\ln \left( \frac{y W D_{c,f_0}^{-\alpha} N_f}{P_c D_{c,c_0}^{-\alpha} T_1} \right)}{\sqrt{\sigma_{c,c_0}^2 + \sigma_{c,f}^2}} \right), \quad (12)$$

where  $H(a) = \int_{-\infty}^a \delta(t) dt$ . Because  $X$  and  $Y$  are independent, the CDF of  $P_{f_0}$  can be derived as

$$F_{P_{f_0}}(p) = \Pr(\min(X, Y) < p) = F_X(p) + F_Y(p) - F_X(p)F_Y(p). \quad (13)$$

Now, (9) can be rewritten as  $SIR_{f,out} = P_{f_0} V$ , where  $V$  is given by

$$V = \frac{\Psi_{f,f_0} D_{f,f_0}^{-\beta}}{\sum_{j=0}^{N_c-1} P_c \Psi_{f,c_j} D_{f,c_j}^{-\alpha}}. \quad (14)$$

Assuming that  $V$  can be approximated by a lognormal RV using Wilkinson's method [22], the probability density function (PDF) of  $V$  can be expressed as

$$f_V(v) = \frac{1}{\sigma_v \sqrt{2\pi v}} \exp \left( -\frac{(\ln(v) - m_v)^2}{\sigma_v^2} \right),$$

$$m_v = \ln \left( \frac{e^{-\sigma_{f,c}^2/2} D_{f,f_0}^{-\beta} \sqrt{\Delta_{f,c_0}}}{P_c W \left( \sum_{j=0}^{N_c-1} D_{f,c_j}^{-\alpha} \right)^2} \right),$$

$$\sigma_V^2 = \ln \left( \frac{e^{\sigma_{f,f_0}^2} \Delta_{fc,0}}{\left( \sum_{j=0}^{N_c-1} D_{f,c_j}^{-\alpha} \right)^2} \right). \quad (15)$$

where  $m_V$  and  $\sigma_V^2$  denote the mean and variance of  $V$  and are expressed using  $\Delta_{fc,0} = \left( e^{\sigma_{f,c}^2} - 1 \right) \sum_{j=0}^{N_c-1} D_{f,c_j}^{-2\alpha}$

+  $\left( \sum_{j=0}^{N_c-1} D_{f,c_j}^{-\alpha} \right)^2$  for brevity.

As  $P_{f_0}$  and  $V$  are independent, the femtocell outage probability in the outer ring with the femtocell SIR requirement  $\gamma_f$  is derived using (13) and (15) as follows:

$$\begin{aligned} P_{o,f,\text{out}} &= \Pr(\text{SIR}_{f,\text{out}} < \gamma_f) \\ &= \int_0^\infty F_{P_{f_0}}(\gamma_f / v | v) f_V(v) dv \\ &= \int_0^\infty F_{P_{f_0}}(\gamma_f / v) f_V(v) dv. \end{aligned} \quad (16)$$

Consider the received SIR for a femtocell user in the inner region. Because the femtocell users in the inner region subtract the interference from the central macrocell BS  $c_0$  from their received signal, the SIR can be expressed as

$$\begin{aligned} \text{SIR}_{f,\text{in}} &= \frac{S_f}{I_{f,c} - I_{f,c_0} + I_{f,c_0,r} + I_{f,f}} \\ &= \frac{P_{f_0} \Psi_{f,f_0} D_{f,f_0}^{-\beta}}{\sum_{j=1}^{N_c-1} P_c \Psi_{f,c_j} D_{f,c_j}^{-\alpha} + \varepsilon \Psi_{f,c_0} D_{f,c_0}^{-\alpha}}, \end{aligned} \quad (17)$$

where the other femtocell interference is ignored for the same reason given in (9). After IC, the residual interference from  $c_0$  is denoted by  $I_{f,c_0,r}$  and is expressed as  $\varepsilon \Psi_{f,c_0} D_{f,c_0}^{-\alpha}$ , where  $\varepsilon$  represents the cancelling error.

The SIR in (17) can be rewritten as  $\text{SIR}_{f,\text{in}} = P_{f_0} U$ , where  $U$  is defined as

$$U = \frac{\Psi_{f,f_0} D_{f,f_0}^{-\beta}}{\sum_{j=1}^{N_c-1} P_c \Psi_{f,c_j} D_{f,c_j}^{-\alpha} + \varepsilon \Psi_{f,c_0} D_{f,c_0}^{-\alpha}}. \quad (18)$$

Because  $U$  approximates a lognormal RV, the PDF of  $U$ ,  $f_U(u)$  is expressed as in (15) with a mean,  $m_U$ , and variance,  $\sigma_U^2$ , where  $m_U$  and  $\sigma_U^2$  are obtained using Wilkinson's method, and the results are omitted [22].

Using the PDF of  $U$ , the femtocell outage probability in the inner region is derived as

$$\begin{aligned} q_{f,\text{in}} &= \Pr(\text{SIR}_{f,\text{in}} < \gamma_f) \\ &= \int_0^\infty F_{P_{f_0}}(\gamma_f / u | u) f_U(u) du, \end{aligned} \quad (19)$$

where  $F_{P_{f_0}}(\gamma_f / u | u)$  is the CDF of the femtocell power,  $P_{f_0}$ , in the inner region conditioned on  $U = u$ . From (8) and (12), the femtocell transmit power in the inner region can be expressed as

$$P_{f_0} = \min \left( X, Y, \frac{I_{f,c_0} T_2}{\Psi_{f,f_0} D_{f,f_0}^{-\beta}} \right), \quad (20)$$

where the same definitions of  $X$  and  $Y$  in (12) are used and we define  $Z$  as

$$Z = \frac{I_{f,c_0} T_2}{\Psi_{f,f_0} D_{f,f_0}^{-\beta}}. \quad (21)$$

Because  $X$ ,  $Y$  and  $Z$  are independent, the conditional CDF of  $P_{f_0}$  in (19) is derived using the CDFs of  $X$ ,  $Y$  and  $Z$  as follows:

$$F_{P_{f_0}}(p | u) = 1 - (1 - F_X(p))(1 - F_Y(p))(1 - F_Z(p | u)), \quad (22)$$

where  $F_X(p)$  and  $F_Y(p)$  are independent of  $U$  and are given in (12). By an approximation of  $Z$  as a lognormal RV, the conditional CDF of  $Z$  can be obtained as follows

$$\begin{aligned} F_Z(p | u) &= 1 - Q \left( \frac{\ln(p) - m_{Z|u}}{\sigma_{Z|u}} \right), \\ m_{Z|u} &= \ln \left( \frac{P_c T_2 e^{-\sigma_{f,c}^2/2} D_{f,c_0}^{-\alpha} \sqrt{\Delta_{fc,\varepsilon} + P_c^2 \Delta_{fc,1}}}{u \left( \varepsilon D_{f,c_0}^{-\alpha} + P_c \sum_{j=1}^{N_c-1} D_{f,c_j}^{-\alpha} \right)^2} \right), \\ \sigma_{Z|u}^2 &= \ln \left( \frac{e^{\sigma_{f,c}^2} (\varepsilon_{fc} + P_c^2 \Delta_{fc,1})}{\left( \varepsilon D_{f,c_0}^{-\alpha} + P_c \sum_{j=1}^{N_c-1} D_{f,c_j}^{-\alpha} \right)^2} \right), \end{aligned} \quad (23)$$

where  $\Delta_{fc,\varepsilon} = \varepsilon D_{f,c_0}^{-\alpha} \left( \varepsilon D_{f,c_0}^{-\alpha} e^{\sigma_{f,c}^2} + 2P_c \sum_{j=1}^{N_c-1} D_{f,c_j}^{-\alpha} \right)$  and

$\Delta_{fc,1} = \left( e^{\sigma_{f,c}^2} - 1 \right) \sum_{j=1}^{N_c-1} D_{f,c_j}^{-2\alpha} + \left( \sum_{j=1}^{N_c-1} D_{f,c_j}^{-\alpha} \right)^2$  are used for

brief expressions. By substituting (23) in (22), the conditional CDF of  $P_{f_0}$  in the inner region is obtained.

Finally, the femtocell outage probability for the inner

region can be calculated from (19).

#### 4.1.2 Macrocell Outage Probability

The macrocell users in the outer region do not share their subchannels with femtocell users. Therefore, no femtocell interference affects the SIR of those macrocell users. The received SIR at the macrocell user can be expressed as

$$\text{SIR}_{c,\text{out}} = \frac{S_c}{I_{c,c}} = \frac{P_c \Psi_{c,c_0} D_{c,c_0}^{-\alpha}}{\sum_{j=1}^{N_c-1} P_c \Psi_{c,c_j} D_{c,c_j}^{-\alpha}}. \quad (24)$$

Considering that  $\text{SIR}_{c,\text{out}}$  in (24) approximates a lognormal RV, the macrocell outage probability in the outer region is derived as

$$\begin{aligned} q_{c,\text{out}} &= \Pr(\text{SIR}_{c,\text{out}} < \gamma_c) \\ &= 1 - Q\left(\frac{\ln(\gamma_c) - m_{c,\text{out}}}{\sigma_{c,\text{out}}}\right), \end{aligned} \quad (25)$$

where  $\gamma_c$  is the macrocell SIR requirement. The mean and variance can be calculated as follows:

$$\begin{aligned} m_{c,\text{out}} &= \ln \left( \frac{e^{-\sigma_{c,c_0}^2/2} D_{c,c_0}^{-\alpha} \sqrt{\Delta_{cc,1}}}{\left(\sum_{j=1}^{N_c-1} D_{c,c_j}^{-\alpha}\right)^2} \right), \\ \sigma_{c,\text{out}}^2 &= \ln \left( \frac{e^{\sigma_{c,c_0}^2} \Delta_{cc,1}}{\left(\sum_{j=1}^{N_c-1} D_{c,c_j}^{-\alpha}\right)^2} \right), \end{aligned} \quad (26)$$

where  $\Delta_{cc,1} = \left(e^{\sigma_{c,c_0}^2} - 1\right) \sum_{j=1}^{N_c-1} D_{c,c_j}^{-2\alpha} + \left(\sum_{j=1}^{N_c-1} D_{c,c_j}^{-\alpha}\right)^2$  is used for concise expressions.

For the macrocell users in the inner region, the sum of the cochannel femtocell interference is limited by the constraint  $I_{c,f} < T_1 P_c \Psi_{c,c_0} D_{c,c_0}^{-\alpha}$  from (8). The received SIR for the macrocell user in the inner region satisfies the following:

$$\begin{aligned} \text{SIR}_{c,\text{in}} &= \frac{S_c}{I_{c,c} + I_{c,f}} \\ &\geq \frac{P_c \Psi_{c,c_0} D_{c,c_0}^{-\alpha}}{\sum_{j=1}^{N_c-1} P_c \Psi_{c,c_j} D_{c,c_j}^{-\alpha} + T_1 P_c \Psi_{c,c_0} D_{c,c_0}^{-\alpha}}. \end{aligned} \quad (27)$$

By considering the restricted femtocell interference, the upper bound for the macrocell outage probability in the inner region can be obtained as

$$\begin{aligned} q_{c,\text{in}} &= \Pr(\text{SIR}_{c,\text{in}} < \gamma_c) \\ &\leq \Pr \left( \frac{\Psi_{c,c_0} D_{c,c_0}^{-\alpha}}{\sum_{j=1}^{N_c-1} \Psi_{c,c_j} D_{c,c_j}^{-\alpha} + T_1 \Psi_{c,c_0} D_{c,c_0}^{-\alpha}} < \gamma_c \right) \\ &= 1 - Q\left(\frac{\ln(\gamma_c) - m_{c,\text{in}}}{\sigma_{c,\text{in}}}\right), \end{aligned} \quad (28)$$

where the mean and variance can be calculated as follows:

$$\begin{aligned} m_{c,\text{in}} &= \ln \left( \frac{e^{-\sigma_{c,c_0}^2/2} D_{c,c_0}^{-\alpha} \sqrt{\Delta_{cc,T_1} + \Delta_{cc,1}}}{\left(T_1 D_{c,c_0}^{-\alpha} + \sum_{j=1}^{N_c-1} D_{c,c_j}^{-\alpha}\right)^2} \right), \\ \sigma_{c,\text{in}}^2 &= \ln \left( \frac{e^{\sigma_{c,c_0}^2} (\Delta_{cc,T_1} + \Delta_{cc,1})}{\left(T_1 D_{c,c_0}^{-\alpha} + \sum_{j=1}^{N_c-1} D_{c,c_j}^{-\alpha}\right)^2} \right), \end{aligned} \quad (29)$$

by letting  $\Delta_{cc,T_1} = T_1 D_{c,c_0}^{-\alpha} \left(T_1 D_{c,c_0}^{-\alpha} e^{\sigma_{c,c_0}^2} + 2 \sum_{j=1}^{N_c-1} D_{c,c_j}^{-\alpha}\right)$ .

#### 4.1.3 Comparisons with the Conventional Scheme

This section compares the outage performances of the proposed scheme with the conventional one. The conventional scheme, in which femtocells reuse the entire spectrum with a fixed transmit power,  $P_{f,\text{max}}$ , is considered because it is the primary scenario in spectrum sharing of two-tier femtocell networks. The received SIR for the femtocell user in the outer ring is expressed as

$$\text{SIR}_{f,\text{conv}} = \frac{P_{f,\text{max}} \Psi_{f,f_0} D_{f,f_0}^{-\beta}}{\sum_{j=0}^{N_c-1} P_c \Psi_{f,c_j} D_{f,c_j}^{-\alpha} + \sum_{i=1}^{M_f-1} P_{f,\text{max}} \Psi_{f,f_i} D_{f,f_i}^{-\alpha}}, \quad (30)$$

where  $M_f$  denotes the number of femtocells per frequency subchannel in the conventional scheme, which satisfies  $M_f \leq N_f$ . The femtocell transmitted power of the proposed scheme is less than  $P_{f,\text{max}}$ , i.e.,  $P_{f_0} \leq P_{f,\text{max}}$  as shown in (8). We find that  $\text{SIR}_{f,\text{out}} \leq \text{SIR}_{f,\text{conv}}$  is satisfied for the femtocell users in the outer region. The possible degradation in the femtocell SIR of the proposed scheme is

the result of restricting the femtocell transmit power to guarantee a high macrocell SIR. On the other hand, because the proposed scheme reuses the subchannels with a high macrocell signal quality ( $S_c$ ), the restriction on the femtocell transmit power can be relieved. Therefore, the degradation in femtocell SIR remains insignificant. The femtocell users in the inner region produces  $SIR_{f,in}$  as (17). In the inner region, the received power from the macrocell BS is dominant and it can be assumed that as  $\varepsilon \Psi_{f,c_0} D_{f,c_0}^{-\alpha} \ll P_c \Psi_{f,c_0} D_{f,c_0}^{-\alpha}$  for the proposed scheme,  $SIR_{f,in} > SIR_{f,conv}$  should hold true in the inner region.

For the macrocell users with the conventional scheme, the received SIR can be expressed as

$$SIR_{c,conv} = \frac{P_c \Psi_{c,c_0} D_{c,c_0}^{-\alpha}}{\sum_{j=1}^{N_c-1} P_c \Psi_{c,c_j} D_{c,c_j}^{-\alpha} + \sum_{i=0}^{M_f-1} P_{f,max} \Psi_{c,f_i} D_{c,f_i}^{-\alpha}}. \quad (31)$$

It is obvious that  $SIR_{c,out} > SIR_{c,conv}$ , which contributes to the protection of the macrocell users from femtocell interference in the outer region. On the other hand, in the inner region,  $SIR_{c,in}$  may be an improvement over  $SIR_{c,conv}$ , depending on the environment. If there are many femtocells,  $SIR_{c,in} > SIR_{c,conv}$  will certainly be achieved because the proposed scheme limits the femtocell interference to a fixed level, irrespective of the number of femtocells.

The femtocell and macrocell outage probabilities for the conventional scheme can be derived in a similar way as  $q_{c,out}$  is derived in Section 4.1.2. The resulting expressions of the per-tier outage probabilities for the conventional scheme are omitted for clarity. Instead, the comparisons of the per-tier outage probability results from the proposed and the conventional schemes are shown in Section 5, which is straightforward from the comparisons of the SIRs.

### 4.2 Total Throughput Analysis

In the previous section, the per-tier SIR and outage performance are analyzed for specific user positions. It is investigated whether the proposed scheme produces an improved SIR over the conventional scheme for individual cases.

In this section, the total throughput performance is investigated to evaluate the proposed scheme. For the investigation, the spatial throughput (ST) is used as a metric. ST is defined as the net number of successful, simultaneous transmissions per frequency subchannel per macrocell site [23].

The ST of the two-tier network employing the proposed spectrum reuse scheme can be expressed as

$$\tau = \max\{ \rho N_f (1 - q_f(r)) + (1 - q_c(r)) \}, 0 < r \leq R_c, \quad (32)$$

where  $q_f(r)$  and  $q_c(r)$  are obtained by averaging the per-

tier outage probabilities of the inner and outer regions over the entire macrocell area, and they are given by  $q_f(r) = E[q_{f,out} | D_{f,c_0} > r] + E[q_{f,in} | D_{f,c_0} < r]$  and  $q_c(r) = E[q_{c,out} | D_{c,c_0} > r] + E[q_{c,in} | D_{c,c_0} < r]$ . In (32), it is assumed that each frequency subchannel is always occupied by a macrocell transmission in a cell site. Among the total frequency subchannels used by the macrocell, only a fraction  $\rho$  of them is occupied by femtocell transmissions. The parameter  $\rho = |B_{in}| / |B|$  denotes the ratio of the number of subchannels in the shared subset  $B_{in}$  to the number of subchannels in the entire set  $B$ , where  $|\cdot|$  measures the size of a set. For a frequency subchannel occupied by femtocells, there are  $N_f$  concurrent femtocell transmissions. From (32), the proposed spectrum reuse scheme can achieve the maximum ST by adjusting  $r$  according to the environment of the two-tier network, while cross-tier interference is effectively limited.

## 5. Numerical Results

This section presents the numerical results achieved using the system parameters listed in Table 1. In each macrocell site,  $N$  femtocells are distributed uniformly. By setting  $T_2$  appropriately, we can ignore the IC error, i.e., we assume  $\varepsilon = 0$  in the simulation [20, 21]. The results from the proposed scheme were compared with the results from the conventional scheme in which the femtocells reuse the entire spectrum with a fixed transmit power,  $P_{f,max}$ .

Fig. 2 shows the total ST obtained using the proposed scheme as a function of  $r$  for different numbers of femtocells and varying maximum femtocell transmit power. The results reveal that there is a single value of  $r$

Table 1. Simulation Parameters.

Symbol	Description	Value
$N_c$	Number of macrocells	19
$R_c, R_f$	Macrocell, femtocell radius	1000, 10 m
$P_c$	Macrocell transmission power	46 dBm
$P_{f,max}$	Maximum femtocell transmit power	20, 10 dBm
$\gamma_c, \gamma_f$	Target SIR	3, 10 dB
$T_1, T_2$	Femtocell power limitation parameters	-10, -10 dB
$W$	Wall penetration loss	-10 dB
$\alpha, \beta$	Path-loss exponent	4, 3
$\sigma_{c,c_0}, \sigma_{f,f_0}, \sigma_{c,c}, \sigma_{c,f}, \sigma_{f,c}, \sigma_{f,f}$	Lognormal shadow parameters	8, 4, 8, 8, 8, 8 dB

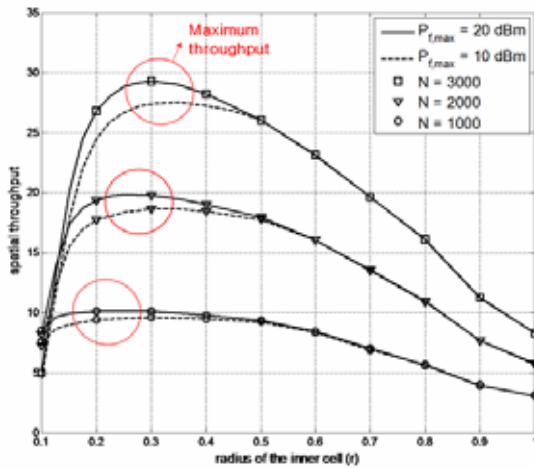


Fig. 2. Total spatial throughput according to the radius  $r$  for different femtocell maximum powers and the number of femtocells per cell site.

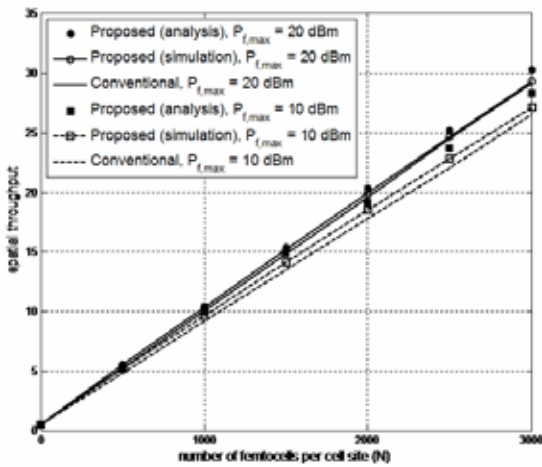


Fig. 3. Total spatial throughput with  $P_{f,max} = 10, 20$  dBm according to the number of femtocells per cell site using  $r$  that maximizes the total spatial throughput

that maximizes the total ST for each  $N$  and  $P_{f,max}$ . If  $r$  is small for a given number of femtocells, the femtocells reuse a very limited spectrum, which results in SIR degradation for both the macrocells and femtocells on the shared spectrum. On the other hand, if  $r$  is large, macrocell subchannels with inferior quality might be reused by femtocells. This also degrades the macrocell and femtocell SIRs and spectral efficiency. As a consequence, the value of  $r$  that maximizes the ST is determined proportionally to the number of femtocells, as shown in Fig. 2. In this figure, the largest value of the optimal  $r$  for all values of  $N$  and  $P_{f,max}$  is less than 0.4. This supports that reusing the limited spectrum consisting of the macrocell subchannels with the superior signal quality is an efficient policy for femtocells in the two-tier network.

Fig. 3 plots the total ST as a function of the number of femtocells per cell site ( $N$ ). The close agreement between

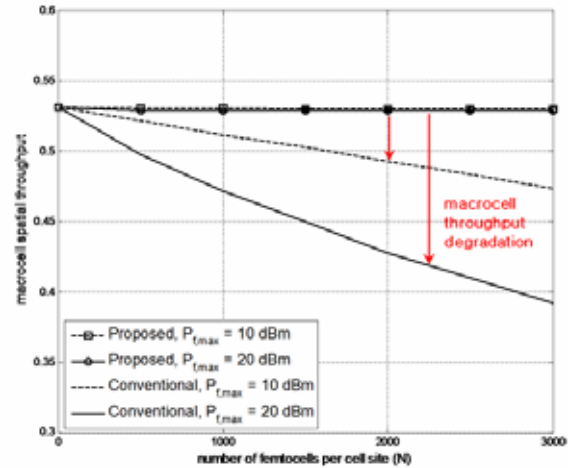


Fig. 4. Macrocell spatial throughput with the max power  $P_{f,max} = 10, 20$  dBm according to the number of femtocells per cell site using  $r$  that maximizes the total spatial throughput.

the analysis and simulation results indicates the accuracy of the analysis of the proposed scheme. This figure shows an almost linear relationship between the total ST and the number of femtocells. This is because the femtocells can operate at much higher spectral efficiencies than their macrocell counterparts and the effect of femtocell interference on femtocell users is negligible in many cases. This figure also confirms that the maximum femtocell power has only a small effect on the ST, i.e., increased femtocell power does not increase the ST, as expected. Considering the femtocell interference to macrocell users, using a low femtocell power level might be beneficial to both the macrocell and femtocell throughput.

Fig. 4 shows the effects of femtocell interference on macrocell throughput by plotting the macrocell ST according to the number of femtocells per cell site. Without any macrocell protection, macrocell throughput degradation is proportional to both the number of femtocells and their transmit power. The proposed spectrum reuse scheme protects the macrocell network successfully from femtocell interference, which results in negligible macrocell throughput degradation for any number of femtocells. To protect the macrocell network, the proposed scheme forces the femtocells to use a limited spectrum and imposes greater power limits than the conventional scheme, but does not cause total throughput loss, as proven in Fig. 3.

Fig. 5 plots the outage probability of the femtocell users according to their distance from the central macrocell BS. This shows the effects of macrocell interference on femtocell users with fixed femtocell interference. With the conventional scheme, near the cell center, no manner of cochannel femtocells can provide a satisfactory QoS; rather, they cause unnecessary interference for other users. On the other hand, using the proposed scheme, we can significantly decrease the femtocell outage probability near the cell center using IC with proper femtocell power curbing in accordance with the SIR analysis in (17).



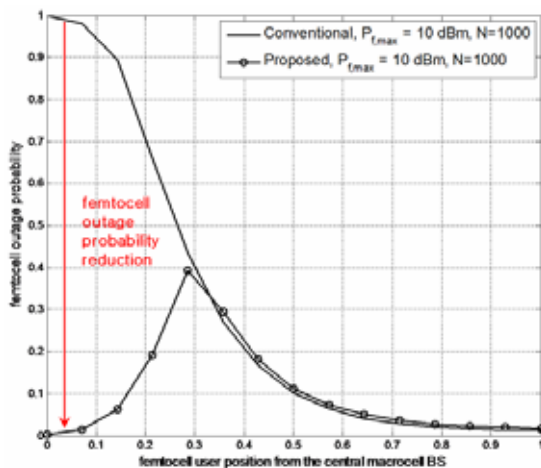


**Fig. 5. Femtocell outage probability with the max power  $P_{f,\max} = 10, 20$  dBm and  $N = 1000$  according to the femtocell user position using  $r$  that maximizes the total spatial throughput**

## 6. Conclusions

This paper proposed a femtocell spectrum reuse scheme to manage the influences of cross-tier interference for macrocells and femtocells that operate in the same spectrum using closed access. Considering the macrocell as the primary infrastructure, the proposed scheme effectively limits the available spectrum and the transmit power of femtocells to ensure a low pre-definable impact on the downlink performance of the macrocell network, and to improve the performance of the femtocell network. The analysis and numerical results prove that femtocells can achieve improved throughput using only a small fraction of the entire spectrum and low transmit power. Consequently, improved total throughput with higher femtocell density of the two-tier network could be achieved while protecting the existing macrocell network.

## References

- [1] V. Chandrasekhar, J. G. Andrews, and A. Gatherer, "Femtocell networks: a survey," *IEEE Commun. Mag.*, vol. 46, pp. 59–67, Sept. 2008. [Article \(CrossRef Link\)](#)
- [2] V. Chandrasekhar, and J. G. Andrews, "Uplink capacity and interference avoidance for two-tier femtocell networks," *IEEE Trans. Wireless Commun.*, vol. 8, pp. 3498–3509, July 2009. [Article \(CrossRef Link\)](#)
- [3] Shu-ping Yeh, S Talwar, Seong-choon Lee, and Heechang Kim, "WiMAX femtocells: a perspective on network architecture, capacity, and coverage," *IEEE Commun. Mag.*, vol. 46, pp. 58–65, Oct. 2008. [Article \(CrossRef Link\)](#)
- [4] Transmission power control schemes for home nodeBs. in 3rd Generation Partnership Project, Tech. Rep. R4-081877. [Article \(CrossRef Link\)](#)
- [5] Youngju Kim, Sungeun Lee, and Daesik Hong, "Performance Analysis of Two-tier Femtocell Networks with Outage Constraints," *IEEE Trans. on Wireless Commun.*, vol. 9, no. 9, pp 2695–2700, Sept. 2010. [Article \(CrossRef Link\)](#)
- [6] H. Claussen, "Performance of macro- and co-channel femtocells in a hierarchical cell structure," in *Proc. IEEE PIMRC*, pp. 1–5, Sept. 2007. [Article \(CrossRef Link\)](#)
- [7] Open and closed access for home nodeBs. in 3rd Generation Partnership Project, Tech. Rep. R4-071231. [Article \(CrossRef Link\)](#)
- [8] V. Chandrasekhar, and J. G. Andrews, "Spectrum allocation in tiered cellular networks," *IEEE Trans. Commun.*, vol. 57, pp. 3059–3068, Oct. 2009. [Article \(CrossRef Link\)](#)
- [9] Prabhu Chandhar, and Suvra Sekhar Das, "Area Spectral Efficiency of Co-Channel Deployed OFDMA Femtocell Networks," *IEEE Trans. on Wireless Commun.*, vol. 13, no. 7, pp 3524–3538, Jul. 2014. [Article \(CrossRef Link\)](#)
- [10] Haining Wang and Zhi Ding, "Macrocell-Queue-Stabilization-Based Power Control of Femtocell Networks," *IEEE Trans. on Wireless Commun.*, vol. 13, no. 9, pp 5223–5236, Sept. 2014. [Article \(CrossRef Link\)](#)
- [11] Xiaohu Ge, Tao Han, Yan Zhang, Guoqiang Mao, Cheng-Xiang Wang, Jing Zhang, Bin Yang, and Sheng Pan, "Spectrum and Energy Efficiency Evaluation of Two-Tier Femtocell Networks With Partially Open Channels," *IEEE Trans. Veh. Technol.*, vol. 63, no. 3, pp. 1306–1319, Mar. 2014. [Article \(CrossRef Link\)](#)
- [12] S. Papavassiliou, L. Tassiulas, and P. Tandon, "Meeting QoS requirements in a cellular network with reuse partitioning," *IEEE J. Sel. Areas Commun.*, vol. 12, no. 8, pp. 1389–1400, Oct. 1994. [Article \(CrossRef Link\)](#)
- [13] A. Pattavina, S. Quadri, and V. Trecordi, "Reuse Partitioning in cellular networks with dynamic channel allocation," in *Proc. IEEE Globecom*, vol. 2, pp. 1543–1548, Nov. 1995. [Article \(CrossRef Link\)](#)
- [14] Eunsung Oh, Myeon-Gyun Cho, Seungyoun Han, Choongchae Woo, and Daesik Hong, "Performance analysis of reuse-partitioning-based subchannelized OFDMA uplink systems in multicell environments," *IEEE Trans. Veh. Technol.*, vol. 57, no. 4, pp. 2617–2621, Jul. 2008. [Article \(CrossRef Link\)](#)
- [15] C. Y. Wong, R. S. Cheng, K. B. Letaief, and R. D. Murch. "Multiuser OFDM with adaptive subcarrier, bit, and power allocation," *IEEE J. Sel. Areas Commun.*, vol. 17, pp. 1747–1758, Oct. 1999. [Article \(CrossRef Link\)](#)
- [16] V. Erceg, L. J. Greenstein, S. Y. Tjandra, S. R. Parkoff, A. Gupta, B. Kulic, A. A. Julius, and R. Bianchi, "An empirically based path loss model for wireless channels in suburban environments," *IEEE J. Sel. Areas Commun.*, vol. 17, no. 7, pp. 1205–1211, Jul. 1999. [Article \(CrossRef Link\)](#)
- [17] V. Chandrasekhar, J. G. Andrews, T. Muharemovic, Z. Shen, and A. Gatherer, "Power control in two-tier femtocell networks," *IEEE Trans. on Wireless*

*Commun.*, vol. 8, no. 8, pp 4316-4328, Aug. 2009.  
[Article \(CrossRef Link\)](#)

- [18] J. Zander and S.-L. Kim. Radio Resource Management for Wireless Networks, 11-50. MA: Artech House, Norwood (2001)
- [19] I. Guvenc, Moo-Ryong Jeong, F. Watanabe, and H. Inamura, "A hybrid frequency assignment for femtocells and coverage area analysis for co-channel operation," *IEEE Commun. Lett.*, vol. 12, pp. 880-882, Dec. 2008. [Article \(CrossRef Link\)](#)
- [20] P. Patel, and J. Holtzman, "Analysis of a simple successive interference cancellation scheme in a DS/CDMA system," *IEEE J. Sel. Areas Commun.*, vol. 12, no. 5, pp. 796-807, Jun. 1994. [Article \(CrossRef Link\)](#)
- [21] J. Andrews, A. Agrawal, T. Meng, and J. Cioffi, "A simple iterative power control scheme for successive interference cancellation," *In Proc. IEEE Int. Symp. Spread Spectrum Techniques, Applications*, vol. 3, pp. 761-765, 2002. [Article \(CrossRef Link\)](#)
- [22] A. A. Abu-Dayya, and N. C. Beaulieu, "Outage probabilities in the presence of correlated lognormal interferers," *IEEE Trans. Veh. Technol.*, vol. 43, no. 1, pp. 164-173, Feb. 1994. [Article \(CrossRef Link\)](#)
- [23] S. Weber, J. G. Andrews, and N. Jindal, "The effect of fading, channel inversion, and threshold scheduling on ad hoc networks," *IEEE Trans. Inf. Theory*, vol. 53, no. 11, pp. 4127-4149, Nov. 2007. [Article \(CrossRef Link\)](#)



**Youngju Kim** received her B.S. and Ph.D. degrees from the School of Electrical and Electronic Engineering, Yonsei university, Seoul, Korea, in 2004 and 2010, respectively. She joined Samsung Electronics in 2010, where she is currently a senior engineer in Modem Development

Laboratory. Her current research interests are in physical layer in wireless communication, especially 3G and 4G systems



**Hanho Wang** received his B.S. and Ph.D. degrees from the School of Electrical and Electronic Engineering, Yonsei university, Seoul, Korea, in 2004 and 2010, respectively. He joined Sangmyung University in 2012, where he is currently an assistant professor in Information and Telecommunication

Engineering. His current research interests are in physical layer in wireless communication, cooperative communications and cognitive radio networks.



**Daesik Hong** received his B.S. and M.S. degrees in Electronics Engineering from Yonsei University, Seoul, Korea, in 1983 and 1985, respectively, and a Ph.D. degree from the School of EE, Purdue University, West Lafayette, IN, in 1990. He joined Yonsei University in 1991, where he is currently a Professor with the School of Electrical and Electronic Engineering. He was Chair of Samsung-Yonsei Research Center for Mobile Intelligent Terminals. He also served as a Vice-President of Research Affairs and a President of Industry-Academic Cooperation Foundation, Yonsei University, from 2010 to 2011. He was also a Chief Executive Officer (CEO) for Yonsei Technology Holding Company in 2011, and served as a Vice-Chair of the Institute of Electronics Engineers of Korea (IEEK) in 2012. Dr. Hong is a senior member of the IEEE. He was an editor of the IEEE Transactions on Wireless Communications from 2006 to 2011. He is currently an editor of the IEEE Wireless Communications Letters. He was appointed as the Underwood/Avison distinguished professor at Yonsei University in 2010, and received the Best Teacher Award at Yonsei University in 2006, 2010, and 2012. He was also a recipient of the Hae-Dong Outstanding Research Awards of the Korean Institute of Communications and Information Sciences (KICS) in 2006 and the Institute of Electronics Engineers of Korea (IEEK) in 2009. His current research activities are focused on future wireless communication including 5G systems, OFDM and multicarrier communication, multi-hop and relay-based communication, cognitive radio, and energy harvesting. More information about his research is available online: <http://mirinae.yonsei.ac.kr>.